Journal of Computational Physics 229 (2010) 2109–2116

Contents lists available at ScienceDirect

Journal of Computational Physics

journal homepage: www.elsevier.com/locate/jcp

Trajectory integration with potential energy discontinuities

Patricia Hurd [a], Teresa Cusati [b], Maurizio Persico [b,*]

[a] Arizona State University, School of Mechanical, Aerospace, Chemical and Materials Engineering, P. O. Box 876106, Tempe, Arizona 85287-6106, USA
[b] Università di Pisa, Dipartimento di Chimica e Chimica Industriale v. Risorgimento 35, I-56126 Pisa, Italy

ARTICLE INFO

Article history:
Received 1 September 2009
Received in revised form 31 October 2009
Accepted 16 November 2009
Available online 20 November 2009

Keywords:
Nuclear trajectories
Discontinuous potentials
Molecular dynamics

ABSTRACT

Many approximate methods of quantum chemistry yield potential energy surfaces with discontinuities. While clearly unphysical, such features often fall within the typical error bounds of the method, and cannot be easily eliminated. The integration of nuclear trajectories when the potential energy is locally discontinuous is obviously problematic. We propose a method to smooth out the discontinuities that are detected along a trajectory, based on the definition of a continuous function that fits locally the computed potential, and is used to integrate the trajectory across the discontinuity. With this correction, the energy conservation error can be reduced by about one order of magnitude, and a considerable improvement is obtained in the energy distribution among the internal coordinates.

1. Introduction

Classical trajectories for the nuclear motion are the basis of molecular dynamics treatments of ground and excited state processes. In this approach the potential energy for the nuclear motion is one of the eigenvalues of the electronic hamiltonian, that depends on the nuclear coordinates as parameters. When a direct strategy is used, the potential energy surface (PES) and its gradient are computed at every time step of the trajectory, i.e. for a given molecular geometry by means of quantum chemistry methods [1–4]. The alternative is to use analytic potential energy functions, either of standard molecular mechanics (MM) type or devised ad hoc for specific systems and processes. The construction of accurate PESs for reaction dynamics and/or multistate processes can be a complex problem, especially in the case of state degeneracies (conical intersections and crossing seams [5]), and its computational cost increases exponentially with the number of internal coordinates. On the other hand, the cost of direct methods depends linearly on the number and duration of the trajectories, which makes them convenient for the simulation of processes in the picosecond time scale.

One of the drawbacks of the direct use of quantum chemistry methods in trajectory simulations is the possible occurrence of discontinuities in the computed PES. Most methods for the solution of the many-electron problem rely on the variational optimization of non-linear parameters, and may therefore admit several solutions. In other words, the energy, as a function of the electron density or wavefunction parameters, may possess one or more local minima in addition to the global one. If the molecular geometry is varied by small steps, as in trajectory calculations or when scanning a potential energy curve, it is not uncommon to switch from one solution to another one, with a "sudden" change in the electronic energy and in all other properties. Even if the change takes place gradually, but in a very small interval of internal coordinates, it is seen as a discontinuity if one samples the PES by finite time or space steps.

The SCF, DFT and MCSCF methods provide good examples of such behaviour [6–12,4]. In CASSCF, a variant of the general MCSCF approach, the definition of the active space (number of active electrons and orbitals) suffices to determine the global

* Corresponding author.
E-mail address: mau@dcci.unipi.it (M. Persico).

0021-9991/$ - see front matter © 2009 Elsevier Inc. All rights reserved.
doi:10.1016/j.jcp.2009.11.025

minimum. However, swapping an active orbital whose occupation number is close to 0 or 2 with a virtual or doubly occupied orbital, may yield another stable solution of slightly higher energy [10–12]. The particular solution found at a given geometry by the iterative self-consistent procedure depends on many technical details, such as the starting molecular orbitals (MO) and the algorithms that accelerate and/or stabilize the convergence. For instance, the practice of using the MOs of the previous step in a trajectory calculation as the starting point for the SCF or MCSCF procedure may help to maintain a particular solution. However, a solution corresponding to the global minimum for a certain range of molecular geometries, may be just a local minimum at other geometries, and disappear altogether (no minimum) at others yet; in these cases, a sudden switch between two solutions is unavoidable. Configuration Interaction (CI) calculations, of variational or perturbative type, can be based on the SCF or MCSCF MOs in order to improve the treatment of electron correlation. The CI results depend on the MOs, so again they may undergo sudden changes due to switching between different SCF or MCSCF solutions, even if the switch implies a very small change in the SCF or MCSCF energies (a typical case is the conversion from localized to delocalized orbitals). Similar problems are also met with the floating occupation (FO) semiempirical SCF-CI method set up by Granucci et al. [2]. The FO-SCF-CI is an inexpensive alternative to state average (SA) MCSCF for the balanced determination of two or more electronic states, and can be also applied in the ab initio framework [13]. In SA-MCSCF calculations, often used in ab initio multistate molecular dynamics, a further source of discontinuities in the solution is the occurrence of root-switching, i.e. a change in the composition of the subspace of electronic states that are optimized [4]. Notice that root-switching does not affect the FO-SCF-CI results. We end this short overview of possible sources of PES discontinuities, by noting that minor problems are also met in pure MD or in mixed QM/MM treatments, because of cutoffs in the evaluation of small interaction terms or integrals.

The presence of discontinuities in the PES is an unphysical feature, but in many cases cannot be easily eliminated. Two solutions of the electronic problem can be qualitatively and even quantitatively satisfactory, each one in its own range of molecular geometries, and yet not match at intermediate geometries. If the mismatch in the energy of the relevant electronic state does not exceed the typical error of the computational method, it is reasonable to smooth out the discontinuity in order to be able to integrate the trajectories across it. When the PES are prepared beforehand by fitting or interpolation, the discontinuities are automatically smoothed away, and possibly not even noticed. When using the direct approach, one cannot anticipate at which molecular geometry a discontinuity will be met. Even worse, if the convergence of the SCF or MCSCF algorithms is facilitated by using the MOs of the previous trajectory step as a starting point, the switch to another solution is determined by the trajectory itself, the time step, and other technical details. Therefore, we propose a fitting procedure, with a modification of the trajectory integration, to be applied locally when a discontinuity is detected. The mathematical formulation is described in the next section, and the results of tests with a model potential are shown in Section 3.

2. Method

We shall describe a trajectory by n_{var} cartesian coordinates $\mathbf{X}(t)$, functions of time, and the related velocities $\mathbf{V}(t)$. The kinetic and potential energies are also functions of time: $T(t) \equiv T(\mathbf{V}(t))$ and $U(t) \equiv U(\mathbf{X}(t))$. The PES $U(\mathbf{X})$ comes in two sheets, with a discontinuity at the border between them, that we shall call the discontinuity seam. The seam is a set of points of dimension $n_{var} - 1$, whose location in the coordinate space is a priori unknown. The total energy $E = T + U$ should be constant, within the computational accuracy. Several integration methods commonly used, such as those of the Verlet family [14], are based on the PES gradients $\mathbf{G}(\mathbf{X})$ and do not make use of the potential energy values. Therefore, if a trajectory goes through a discontinuity during a time step Δt, the immediate effect is a change in the total energy, from $E(t)$ to $E(t + \Delta t)$, roughly equal to $U(t + \Delta t) - U(t)$. This quantity is in turn an approximation of the exact potential step, $U_D = \lim_{t \to t_D^+} U(t) - \lim_{t \to t_D^-} U(t)$, where t_D is the time at which the trajectory crosses the discontinuity seam (notice that in most practical cases t_D is not easily determined with a resolution better than Δt). The discontinuity is therefore detected by checking the energy conservation, as usually done to test the accuracy of the integration. Of course, across the same time step the gradient is also expected to change more or less abruptly, and the gradient discontinuity is also detrimental to the integration accuracy. In some cases one may accidentally find $U(t + \Delta t) \simeq U(t)$, in spite of switching between two different solutions of the electronic problem. Then, the comparison of the two gradients at $X(t)$ and $X(t + \Delta t)$ can be useful to detect the discontinuity, when the energy criterium fails. Therefore, we shall apply the smoothing procedure described below, whenever two successive time steps t and $t + \Delta t$ yield

$$|E(t + \Delta t) - E(t)| > E_{thresh} \tag{1}$$

or

$$|\mathbf{G}(t + \Delta t) - \mathbf{G}(t)|^2 / |\mathbf{X}(t + \Delta t) - \mathbf{X}(t)|^2 > G_{thresh} \tag{2}$$

In all the tests we have performed, the two thresholds were set to $E_{thresh} = 0.0002$ a.u. and $G_{thresh} = 2$ a.u.

Note that the energy conservation could be enforced by simply resetting the kinetic energy to $T'(t + \Delta t) = T(t) + U(t) - U(t + \Delta t)$. However, this simple recipe does not define univocally the corrected velocity vector. Moreover, when $U(t + \Delta t) - U(t) > T(t)$ it cannot be applied. This is why we propose a slightly more elaborated procedure. We define a fitting function $F(\mathbf{X})$, with continuous first derivatives, connecting two points of the trajectory, $\mathbf{X}_1 = \mathbf{X}(t_1)$ and $\mathbf{X}_2 = \mathbf{X}(t_2)$, at the opposite sides of the discontinuity. $F(\mathbf{X})$ must approximate the computed PES $U(\mathbf{X})$ in the neighborhoods of

both $\mathbf{X}_1$ and $\mathbf{X}_2$, so we shall require $F(\mathbf{X})$ to have the same values and gradients as $U(\mathbf{X})$ in these two points. The integration of the trajectory for the time interval $[t_1, t_2]$ will be repeated, using $F(\mathbf{X})$ as the potential energy function, and then we shall switch again to the true PES $U(\mathbf{X})$. Of course, after time t_1 and geometry $\mathbf{X}_1$ the trajectory will be altered, and in general the point $\mathbf{X}_2'$ obtained at time t_2 will differ from $\mathbf{X}_2$. Because of this fact, the algorithm is not time-reversible.

In order to bridge the discontinuity, that is known to occur between the times t and $t + \Delta t$, we must choose $t_1 \leqslant t$ and $t_2 \geqslant t + \Delta t$. The simplest possibility is $t_1 = t$ and $t_2 = t + \Delta t$ ("one-step" procedure), but we prefer to choose two points further from the discontinuity for two reasons. One is that, near the discontinuity, many quantum chemistry methods may undergo numerical problems, and yield inaccurate energies and gradients. In fact, note that either $\mathbf{X}(t)$ or $\mathbf{X}(t + \Delta t)$ may lie accidentally very close to the discontinuity. There is a second reason against setting $t_2 = t + \Delta t$: with $\mathbf{X}_2$ near the discontinuity, the neighborhood of $\mathbf{X}_2$ where $F(\mathbf{X})$ approximates well $U(\mathbf{X})$ would have a sharp boundary very close to $\mathbf{X}_2$, and the point $\mathbf{X}_2'$ may easily fall outside this region. This situation is illustrated in Fig. 1. In such conditions, resuming the integration with the $U(\mathbf{X})$ potential leads to large errors, as we have observed in a set of tests described in the next section. Our standard choice is therefore: $\mathbf{X}_1 = \mathbf{X}(t - \Delta t)$ and $\mathbf{X}_2 = \mathbf{X}(t + 2\Delta t)$. The latter point is obtained by propagating the trajectory for one time step more, after detecting the discontinuity, with the $U(\mathbf{X})$ potential. Fig. 1 depicts the basic elements of this "three-step" procedure for a one-dimensional case.

The function $F(\mathbf{X})$ must obey $2(n_{var} + 1)$ conditions:

$$\begin{aligned} F(\mathbf{X}_1) &= U(\mathbf{X}_1) \\ F(\mathbf{X}_2) &= U(\mathbf{X}_2) \\ \left(\frac{\partial F}{\partial \mathbf{X}}\right)_{\mathbf{X}=\mathbf{X}_1} &= \mathbf{G}(\mathbf{X}_1) \\ \left(\frac{\partial F}{\partial \mathbf{X}}\right)_{\mathbf{X}=\mathbf{X}_2} &= \mathbf{G}(\mathbf{X}_2) \end{aligned} \tag{3}$$

We shall adopt a general expression of the form

$$F(\mathbf{X}) = [1 - S(\alpha)]\ [U_1 + \mathbf{G}_1^t(\mathbf{X} - \mathbf{X}_1)] + S(\alpha)\ [U_2 + \mathbf{G}_2^t(\mathbf{X} - \mathbf{X}_2)] \tag{4}$$

Here α is the advancement coordinate

$$\alpha = \frac{(\mathbf{X}_2 - \mathbf{X}_1)^t(\mathbf{X} - \mathbf{X}_1)}{|\mathbf{X}_2 - \mathbf{X}_1|^2} \tag{5}$$

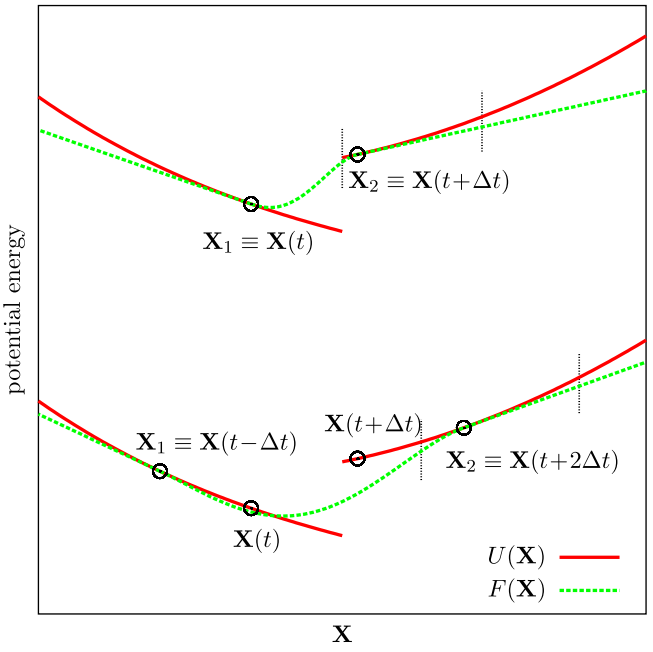

Fig. 1. Schematic illustration of the method. The lower curves represent our standard "three-step" procedure, whereby we define the F function with reference to the points $\mathbf{X}_1 = \mathbf{X}(t - \Delta t)$ and $\mathbf{X}_2 = \mathbf{X}(t + 2\Delta t)$. The upper curves show an unfavorable case for the "one-step" procedure, with $\mathbf{X}_1 = \mathbf{X}(t)$ and $\mathbf{X}_2 = \mathbf{X}(t + \Delta t)$. The vertical bars show the range of coordinates where the function $F(\mathbf{X})$ approximates well the potential $U(\mathbf{X})$, i.e. where $|F(\mathbf{X}) - U(\mathbf{X})|$ does not exceed 1/10 of the potential step.

and $S(\alpha)$ is the sigmoid function

$$S(\alpha) = \begin{cases} 0 & \text{for } \alpha \leqslant 0 \\ 3\alpha^2 - 2\alpha^3 & \text{for } 0 \leqslant \alpha \leqslant 1 \\ 1 & \text{for } \alpha \geqslant 1 \end{cases} \tag{6}$$

The constraints (3) are satisfied by choosing

$$\begin{aligned} U_1 &= U(\mathbf{X}_1) \\ U_2 &= U(\mathbf{X}_2) \\ \mathbf{G}_1 &= G(\mathbf{X}_1) \\ \mathbf{G}_2 &= G(\mathbf{X}_2) \end{aligned} \tag{7}$$

With a substantial potential step U_D we have $U_2 - U_1 \simeq U_D$, so the gradient of $F(\mathbf{X})$ will be largest around the midpoint $(\mathbf{X}_1 + \mathbf{X}_2)/2$, and will point approximately in the direction $\mathbf{X}_2 - \mathbf{X}_1$. The complete expression of the gradient of $F(\mathbf{X})$, that is used to integrate Newton's equations, is

$$\frac{\partial F}{\partial X_r} = \left[U_2 - U_1 - \mathbf{G}_1^t(\mathbf{X} - \mathbf{X}_1) + \mathbf{G}_2^t(\mathbf{X} - \mathbf{X}_2)\right] \frac{\partial S}{\partial \alpha} \frac{\partial \alpha}{\partial X_r} + [1 - S(\alpha)]\mathbf{G}_1 + S(\alpha)\mathbf{G}_2 \tag{8}$$

with

$$\frac{\partial \alpha}{\partial X_r} = \frac{X_{2,r} - X_{1,r}}{|\mathbf{X}_2 - \mathbf{X}_1|^2} \tag{9}$$

and

$$\frac{\partial S}{\partial \alpha} = 6(\alpha - \alpha^2) \quad \text{for} \quad 0 \leqslant \alpha \leqslant 1 \tag{10}$$

while $dS/d\alpha = 0$ outside this interval.

To integrate the trajectories we made use of the velocity Verlet algorithm [14], which allows for calculation of the potential and kinetic energies at the same time and only needs the positions and velocities at a given time t to propagate them at $t + \Delta t$. Our conclusions, however, are largely independent on the integration algorithm as long as the time step is small enough to guarantee a sufficient accuracy. The integration from time $t_1 = t - \Delta t$ and position $\mathbf{X}_1$, to $t_2 = t + 2\Delta t$ and $\mathbf{X}_2'$ is done with a time step $\Delta t'$ smaller than Δt, because the fitting potential $F(\mathbf{X})$ can be considerably steeper than $U(\mathbf{X})$, and because in real applications it does not imply time-consuming quantum chemistry calculations. In some preliminary tests with the model potentials used in the next section we found that a 20-fold reduction of the time step ($\Delta t' = \Delta t/20$) was more than sufficient, so it was adopted throughout the other tests. When resuming the integration with the $U(\mathbf{X})$ potential at t_2 and $\mathbf{X}_2'$, we calculate the exact $U(\mathbf{X}_2')$ and $\mathbf{G}(\mathbf{X}_2')$ quantities, instead of using the approximate values given by $F(\mathbf{X})$.

3. Tests with a model potential

We ran several tests with the model potential

$$U(\mathbf{X}) = Ae^{-BX_1} + V_D\, H(X_1 - X_D) + \sum_{r=2}^{n_{var}} C_r\, [X_r - H_D\, H(X_1 - X_D)]^2 \tag{11}$$

where $H(X)$ is the Heaviside function. The discontinuity is found at $X_1 = X_D$, and has a "vertical" and a "horizontal" component, V_D and H_D, respectively. Most of the tests were done with the following values of the parameters: $A = 0.08,\ B = 0.3,\ C_r = 0.20, X_D = 6$, all in atomic units. The mass was $M = 20,000$ a.u. (same for all the coordinates). With this form of the discontinuity the exact solution is easily computed, using the reflection and refraction laws. The discontinuity seam is perpendicular to the X_1 direction, so only V_1 is affected. When the U_D step is positive and larger than the $T_1 = MV_1^2/2$ component of the kinetic energy, the trajectory is reflected, i.e. the sign of V_1 is reversed. When $U_D < T_1$, the velocity V_1 is changed to $V_1' = \sqrt{V_1^2 - 2U_D/M}$. Notice that in practical applications the exact position and orientation of the seam are unknown, so the reflection and refraction laws cannot be applied. Thanks to the simplicity of the model potential, we were able to test the procedure described in the previous section versus the exact theory.

Each test consisted of 500 trajectories, with initial coordinates and velocities sampled according to Gaussian distributions. For the X_1 coordinate, the Gaussian was centered at $\langle X \rangle = 3$ a.u., with the standard deviation $\sigma_X = 0.5$ a.u., and for all the other coordinates we had $\langle X \rangle = 0$ and $\sigma_X = 0.2$ a.u. The velocities were centered at $\langle V \rangle = 0$, with $\sigma_V = 0.0005$ a.u. Different values of σ_X and σ_V were used in particular cases. The trajectories were stopped at $t_{max} = 10000$ a.u. (about 250 fs) and the standard time step was 10 a.u. (about 0.25 fs). Table 1 shows a selection of results, with different choices of the physical and numerical parameters.

Table 1
Results of some selected tests. All quantities in a.u., energies in mH (10^{-3} a.u.). The U_D column reports the average and standard deviation of the largest potential step found along each trajectory. The ΔE and ΔE_1 columns report the energy conservation and energy transfer errors (averages and standard deviations). The "beyond disc." column reports the percentage of trajectories that end beyond the discontinuity ($X_1(t_{max}) > 6$ a.u.) and the error with respect to exact calculations (in parenthesis). Unless stated otherwise in the first column, the tests are made with $n_{var} = 2,\ H_D = 0.10$ a.u., $V_D = 0,\ M = 20,000$ a.u., $C_r = 0.2$ a.u., $\Delta t = 10$ a.u..

tested parameter	H_D	V_D	U_D	ΔE	ΔE_1	Beyond disc. (%)
V_D	0	−20	−20.00 ± 0.00	0.00 ± 0.00	−2.88 ± 3.23	100.0 (0)
	0	−10	−10.00 ± 0.00	0.00 ± 0.00	−1.44 ± 1.62	100.0 (0)
	0	10	10.00 ± 0.00	0.34 ± 0.23	1.75 ± 1.51	100.0 (0.4)
	0	20	20.00 ± 0.00	2.42 ± 1.65	5.02 ± 2.88	99.2 (42.0)
H_D	0.050	0	0.34 ± 3.40	0.01 ± 0.06	0.04 ± 0.77	100.0 (0)
	0.100	0	1.68 ± 6.81	0.14 ± 0.50	0.08 ± 1.98	100.0 (1.4)
	0.150	0	4.01 ± 10.21	0.42 ± 1.41	−0.36 ± 4.04	100.0 (6.4)
	0.200	0	7.35 ± 13.61	0.85 ± 3.14	−1.90 ± 6.70	99.6 (16.2)
$n_{var} = 3$[a]	0.071	0	1.61 ± 6.70	0.09 ± 0.43	0.30 ± 2.53	100.0 (1.0)
$n_{var} = 6$	0.045	0	1.82 ± 6.42	0.04 ± 0.15	0.74 ± 3.29	100.0 (1.2)
$n_{var} = 15$	0.027	0	2.08 ± 6.32	0.00 ± 0.07	1.25 ± 4.39	100.0 (1.4)
$n_{var} = 48$	0.015	0	1.77 ± 6.40	−0.06 ± 0.03	1.47 ± 5.62	100.0 (0.8)
$C_r = 0.01$[b]	0.447	0	2.16 ± 6.84	0.15 ± 0.49	0.22 ± 2.21	100.0 (1.6)
$C_r = 0.05$	0.200	0	2.23 ± 6.82	0.18 ± 0.61	0.02 ± 2.66	100.0 (1.8)
$C_r = 2.00$	0.032	0	2.22 ± 6.54	0.14 ± 0.51	0.22 ± 2.22	100.0 (1.0)
$M = 2000$[c]	0.150	0	1.67 ± 6.83	0.14 ± 0.48	0.13 ± 1.93	100.0 (0.4)
$M = 100,000$[d]	0.150	0	1.68 ± 6.80	0.14 ± 0.49	0.07 ± 1.99	100.0 (1.6)
$\Delta t = 1$	0.150	0	1.68 ± 6.80	0.10 ± 0.71	0.08 ± 1.97	100.0 (1.4)
$\Delta t = 50$	0.150	0	1.70 ± 6.84	0.07 ± 0.62	0.11 ± 2.06	100.0 (1.4)
One-step, $\Delta t = 10$	0.150	0	1.68 ± 6.81	−0.30 ± 1.90	−0.14 ± 2.43	99.6 (1.8)
one-step, $\Delta t = 30$	0.150	0	1.69 ± 6.85	−0.25 ± 1.84	−0.16 ± 2.17	100.0 (1.4)

[a] The horizontal discontinuity H_D scales as $(n_{var} - 1)^{-1/2}$: $H_D = 0.10/\sqrt{n_{var} - 1}$.
[b] The horizontal discontinuity H_D and the gaussian width for the X_2 initial conditions scale as $C_r^{-1/2}$: $H_D = 0.10\sqrt{0.20/C_r},\ \sigma_X = 0.20\sqrt{0.20/C_r}$.
[c] The gaussian width for the velocity initial conditions scales as $M^{-1/2}$: $\sigma_V = 0.0005\sqrt{20,000/M}$.
[d] The time t_{max} is extended to 20,000 a.u., so that all trajectories go through the discontinuity in spite of the slower dynamics.

We tested the internal consistency of the method under two different aspects. First, we have evaluated the performance of our procedure in the absence of discontinuities ($H_D = 0$ and $V_D = 0$), by forcing its use when a trajectory crosses the $X_1 = X_D$ threshold. In this case one would like to obtain the same trajectory by using $U(\mathbf{X})$ or $F(\mathbf{X})$, i.e. $\mathbf{X}'_2 = \mathbf{X}_2$. We computed the relative error $|\mathbf{X}'_2 - \mathbf{X}_2|/|\mathbf{X}_2 - \mathbf{X}_1|$ with the standard parameters given above, and we obtained a root mean squared (RMS) value of 2.5×10^{-4}. This small error is partly due to the inaccuracy of the fitting potential and partly to the use of two different time steps Δt and $\Delta t'$ in computing $\mathbf{X}_2$ and $\mathbf{X}'_2$. In fact, by using $\Delta t' = \Delta t = 10$ a.u. the RMS relative error is reduced to 1.6×10^{-4}. Another required feature is the invariance under rotations of the coordinate system, which means the results must be independent on the molecular orientation. This is warranted by the fact that the fitting function $F(\mathbf{X})$ is defined in terms of scalars and vectors with the correct transformation properties under rotations. A change in the coordinate system only affects the numerics. To test this point, we rotated the X_1 and X_2 axes by an arbitrary angle, so that the exponential term and the first harmonic term in the model potential depend on both coordinates. With a rotated potential, and consistently rotated initial conditions, we obtain the same results of Table 1.

To test the accuracy of the method, besides the energy conservation, we also considered the final energy partition among the n_{var} coordinates. Without the horizontal discontinuity, i.e. when $H_D = 0$, the $U(\mathbf{X})$ potential is separable into a sum of single coordinate terms U_r, namely the exponential term plus the vertical discontinuity term for the X_1 coordinate, and the harmonic terms for $r \geqslant 2$. Then, the total energy can be partitioned into time-independent components $E_r = U_r + T_r$. The horizontal discontinuity brings about an energy transfer between X_1 and the other coordinates, but the E_r energy components are still constant before and after the discontinuity. Our general procedure, not tailored to a specific form of the potential, can deviate from the theoretical energy partition. We shall therefore monitor the error in E_1, i.e. the computed final E_1 minus its exact value obtained by the reflection and refraction laws: $\Delta E_1 = E_{1,comp}(t_{max}) - E_{1,exact}(t_{max})$. The error in the total energy is instead an internal test: $\Delta E = E(t_{max}) - E(0)$.

The single parameter with the largest effect on the accuracy appears to be the U_D potential step. When the discontinuity is only vertical ($H_D = 0, V_D \neq 0$), U_D is the same for all trajectories and coincides with V_D. This simple case is illustrated in Fig. 2 (see also Table 1), where we plot the average and the standard deviation of the errors in the total energy, ΔE, and in the E_1 component, ΔE_1. Negative discontinuities $U_D < 0$ do not affect the energy conservation, and good results are obtained also with positive U_D, up to 10–15 mH (1 mH $\equiv 10^{-3}$ a.u.). The ΔE_1 error is larger, i.e. a certain amount of energy transfer takes place, which is an artifact not fully eliminated by the proposed procedure. In this example as in all the following ones, one should consider that, without corrections, both ΔE and ΔE_1 would be approximately the same as U_D. We see that our algorithm reduces ΔE by more than one order of magnitude and ΔE_1 by a factor 5, for V_D up to 15 mH. With positive V_D, a fraction

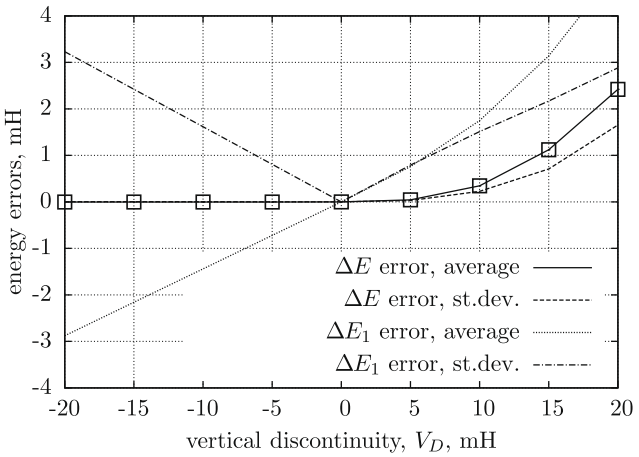

Fig. 2. Averages and standard deviations of the error on the total energy, ΔE, and on the E_1 component, ΔE_1, as functions of the vertical discontinuity parameter V_D.

of the trajectories should be reflected by the discontinuity and should end up with $X_1(t_{max}) < X_D$. In fact, this fraction is very small up to $V_D = 0.10$, but it increases sharply beyond $V_D = 0.15$. Our procedure fails to reproduce this result, because some energy is transferred from the other coordinates to X_1 and allows the particle to overcome the barrier.

With a horizontal discontinuity, the potential step U_D depends on the trajectory. It can be positive or negative, but the average is always positive and proportional to H_D^2 (see Table 1). Fig. 3 shows the single trajectory ΔE values versus U_D. Again we see that the energy is conserved with good accuracy with negative or small positive U_D. For $U_D > 10$ mH, only a minority of the trajectories yield unacceptably large errors ($\Delta E > 1$ mH). The energy conservation error is essentially due to the difference between $\mathbf{X}_2'$ (ending point of the integration with the $F(\mathbf{X})$ potential) and $\mathbf{X}_2$ (reference point to define thr $F(\mathbf{X})$ function). The further is $\mathbf{X}_2'$ from $\mathbf{X}_2$, the larger the difference $U(\mathbf{X}_2') - F(\mathbf{X}_2')$, i.e. in practice ΔE.

The energy transfer error is instead influenced by the ratio of the velocity components parallel and perpendicular to the discontinuity seam, $\mathbf{V}_\parallel$ and $\mathbf{V}_\perp$. In fact, only the kinetic energy associated with $\mathbf{V}_\perp$ should change, by the amount $-U_D$. However, the function $F(\mathbf{X})$ has the steepest variation in the $\mathbf{V}$ direction, i.e. along the α variable (remember that in practical applications $\mathbf{V}$ is known, while $\mathbf{V}_\perp$ is not). So, a fraction $\mathbf{V}_\parallel^2/\mathbf{V}^2$ of the kinetic energy change $-U_D$ is attributed to the other coordinates and is found missing from the E_1 energy component. As shown in Fig. 4, the energy transfer error ΔE_1 correlates very well with $U_D\mathbf{V}_\parallel^2/\mathbf{V}^2$. In all our tests (see Table 1) ΔE_1 appears to be statistically smaller than U_D, i.e. the total error that would be observed in the absence of corrective treatments. The average error is much smaller than the standard deviation, except in the case of a purely vertical discontinuity. In particular, Fig. 5 shows that the results obtained by varying the horizontal discontinuity parameter are quite acceptable up to $H_D \simeq 0.12$ a.u.

In the tests with more than two variables, the horizontal discontinuity H_D was scaled down by the factor $\sqrt{n_{var} - 1}$, in order to keep the average potential step U_D approximately constant. The energy conservation improves with the number

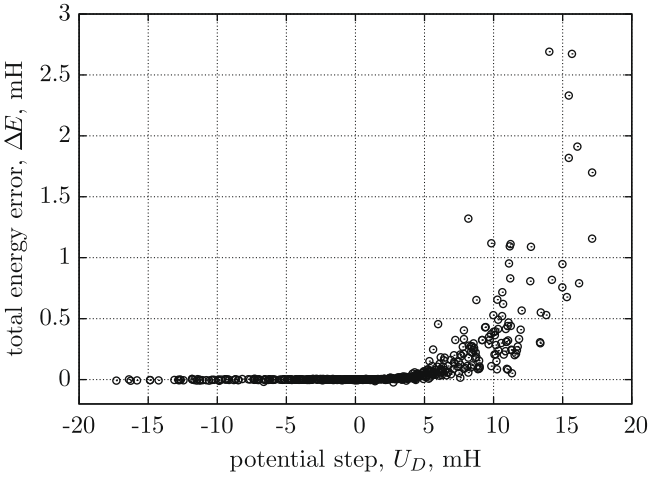

Fig. 3. Error on the total energy, ΔE, versus the potential step U_D, for an horizontal discontinuity $H_D = 0.1$ a.u.

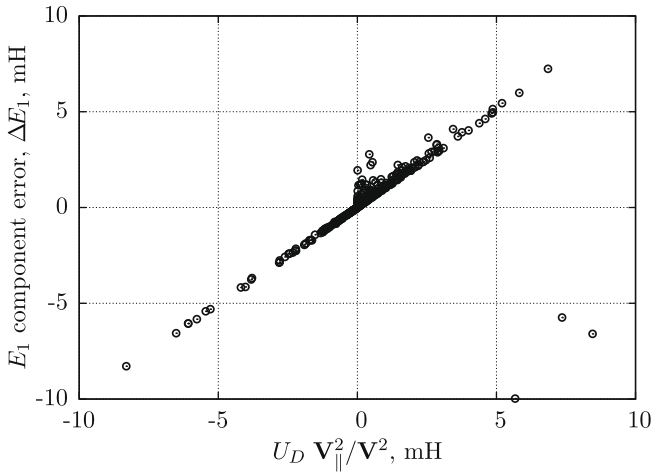

Fig. 4. Error on the E_1 energy component, ΔE_1, versus the potential step U_D times $\mathbf{V}_\parallel^2/\mathbf{V}^2$, where $\mathbf{V}_\parallel$ is the component of the velocity vector parallel to the discontinuity seam. Horizontal discontinuity, $H_D = 0.10$ a.u.

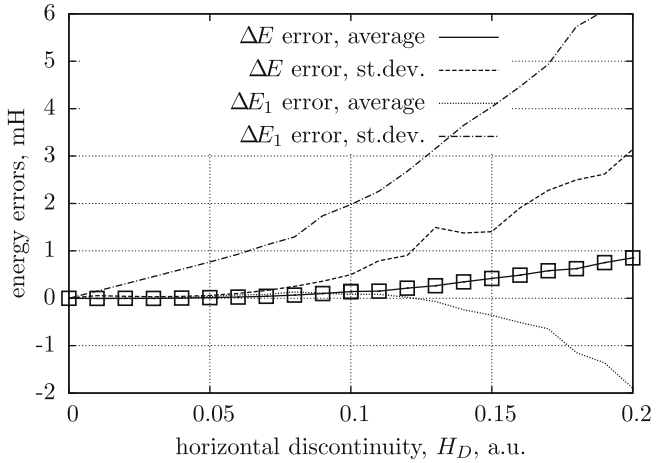

Fig. 5. Averages and standard deviations of the error on the total energy, ΔE, and on the E_1 component, ΔE_1, as functions of the horizontal discontinuity parameter H_D.

of variables, while the energy transfer error gradually increases, which is consistent with its origin as discussed above. For very large systems, it seems therefore advisable to restrict the definition of the α variable to a subset of important coordinates: for instance, the H atoms that undergo high frequency and small amplitude vibrations, or the MM atoms in mixed QM/MM treatments, could be excluded. To test this idea, we changed the definition of α, Eq. (5), to $\alpha = (X_r - X_{1,r})/(X_{2,r} - X_{1,r})$ with $r = 1$, dropping all the coordinates with $r > 1$. In the $n_{var} = 48$ run reported in Table 1, this change reduced the energy transfer error to 0.04 ± 1.20 mH. Notice however that in real applications one would need at least a qualitative identification of the relevant coordinates.

In two more sets of tests we have varied the force constant C_2 and the mass M. In order to keep the average potential energy $\langle U(t=0)\rangle$ and the potential step $\langle U_D\rangle$ approximately constant, we have scaled the horizontal discontinuity H_D and the gaussian width for the X_2 initial conditions as $C_2^{-1/2}$: $H_D = 0.10\sqrt{0.20/C_2}$, $\sigma_X = 0.20\sqrt{0.20/C_2}$. Similarly, to avoid changing the kinetic energy and the amplitude of the oscillation, we have scaled the width for the velocity initial conditions as $M^{-1/2}$: $\sigma_V = 0.0005\sqrt{20,000/M}$. With these provisions, the accuracy of the results is apparently not sensitive to the force constant, nor to the mass (see again Table 1).

In the last rows of Table 1 we show the results of more technical tests. The time step Δt parameter can be varied over a considerable range of values, without substantially affecting the results. Note that the definition of the $F(\mathbf{X})$ function is affected by the time-step, mainly through the $\mathbf{X}_2 - \mathbf{X}_1$ vector and the advancement coordinate α (see Eqs. (4)–(6)). The function $S(\alpha)$ has derivatives of order n with respect to the $\mathbf{X}_2 - \mathbf{X}_1$ direction roughly proportional to Δt^{-n} (with $n \leqslant 3$). Larger values of the higher order derivatives ($n > 1$) could be detrimental to the accuracy of the trajectory integration, but the concurrent reduction of the time-step (further decreased when using the fitting function) offsets this effect. We also tested the one-step

procedure, that yielded larger energy conservation errors with respect to the standard three-step one (see the last two rows of Table 1). In one test we used the same $\Delta t = 10$ a.u. as in the three-step case, and in the other one we set $\Delta t = 30$ a.u., so that the time interval for the definition of the $F(\mathbf{X})$ function, $t_2 - t_1$, is the same as in the three-step procedure. Notice that, even in the latter case, it is possible that either $\mathbf{X}_1$ or $\mathbf{X}_2$ lie very close to the discontinuity (see previous section and Fig. 1).

4. Concluding remarks

We have proposed a simple procedure to deal with small discontinuities in the potential energy, in trajectory simulations of the molecular dynamics. Such discontinuities may occur when solving the electronic problem "on the fly", with quantum chemistry methods, during the integration of the nuclear trajectory. They are often under the "chemical" accuracy, i.e. one or a few kcal/mol, depending on the problem.

Our procedure consists of smoothing out a discontinuity by replacing the potential computed "on the fly" with a simple function of the nuclear coordinates for a short stretch of the trajectory. We have tested the algorithm on a model potential, monitoring both the total energy conservation and the energy transfer between different coordinates. We have run tests with two different types of sudden changes in the model potential, and we have varied the extent of the discontinuity, a few other potential parameters, and some numerical parameters and options. The method reduces the error on the total energy by one order of magnitude, and the error on the energy distribution among different modes by a smaller but quite significant factor, with respect to uncorrected trajectories. The single factor with the largest influence on the accuracy of the algorithm is the potential energy step U_D. Another important factor is the angle between the direction of the trajectory and the discontinuity seam: small angles can favour a spurious energy transfer between different coordinates. Notice however that, while U_D is easily evaluated during the integration of a trajectory, the orientation of the discontinuity seam and therefore the angle are unknown. In practical applications, good results are expected with U_D not exceeding a few mH (1 mH = 10^{-3} a.u. = 0.6275 kcal/mol), which is the range of discontinuities usually tolerated on chemical accuracy grounds.

Acknowledgments

We are grateful to Professor Yu Zhuang, of Texas Tech University, for very helpful discussions. Most of this work has been carried out in Pisa, during the "Summer Abroad Program 2009" of the NSF-PIRE project "Simulation of Electronic Non-Adiabatic Dynamics for Reactions with Macromolecules, Liquids, and Solids", of which one of us (P.H.) was one of the selected participants.

References

[1] T. Vreven, F. Bernardi, M. Garavelli, M. Olivucci, M.A. Robb, H.B. Schlegel, J. Am. Chem. Soc. 119 (1997) 12687.
[2] G. Granucci, M. Persico, A. Toniolo, J. Chem. Phys. 114 (2001) 10608.
[3] M. Barbatti, G. Granucci, M. Persico, M. Ruckenbauer, M. Vazdar, M. Eckert-Maksic, H. Lischka, J. Photochem. Photobiol. A 190 (2007) 228.
[4] J.M. Hostettler, A. Bach, P. Chen, J. Chem. Phys. 130 (2009) 034303.
[5] M. Persico, Electronic diabatic states: definition, computation and applications, in: P.v.R. Schleyer, N.L. Allinger, T. Clark, J. Gasteiger, P.A. Kollman, H.F. Schaefer III, P.R. Schreiner (Eds.), Encyclopedia of Computational Chemistry, Wiley, Chichester, 1998, p. 852.
[6] J.S. Sears, C.D. Sherrill, J. Chem. Phys. 124 (2006) 144314.
[7] A.J. Thom, M. Head-Gordon, Phys. Rev. Lett. 101 (2008) 193001.
[8] S. Goel, A.E. Masunov, J. Chem. Phys. 129 (2008) 214302.
[9] X. Li, J. Paldus, J. Chem. Phys. 130 (2009) 084110.
[10] R. Shepard, in: G.L. Malli (Ed.), Relativistic and Electron Correlation Effects in Molecules and Solids, Plenum, New York, 1994, p. 161.
[11] C. Angeli, C.J. Calzado, R. Cimiraglia, S. Evangelisti, D. Maynau, Mol. Phys. 101 (2003) 1937.
[12] S. Yamamoto, H. Tatewaki, H. Moriyama, H. Nakano, J. Chem. Phys. 124 (2006) 124302.
[13] A. Toniolo, M. Persico, D. Pitea, J. Chem. Phys. 112 (2000) 2790.
[14] A.K. Mazur, J. Comput. Phys. 136 (1997) 354.